Design, Analysis, and Real Time Simulation of a 3D Soft Robotic Snake

Zhenyu Wan,[*] Yinan Sun,[*] Yun Qin, Erik H. Skorina,
Renato Gasoto, Ming Luo, Jie Fu, and Cagdas D. Onal[†‡]

Abstract

Snakes are a remarkable source of inspiration for mobile search-and-rescue robots. Their unique slender body structure and multiple modes of locomotion are well-suited to movement in narrow passages and other difficult terrain. The design, manufacturing, modeling, and control techniques of soft robotics make it possible to imitate the structure, mechanical properties, and locomotion gaits of snakes, opening up new possibilities in robotics research. Building on our track record of contributions in this area, this paper presents a soft robotic snake made of modules that can actively deform in 3-D and rigorously studies its performance under a range of conditions, including gait parameters, number of modules, and differences in the environment. A soft 3D-printed wave-spring sheath is developed to support the robot modules, increasing the snake's performance in climbing steps three-fold. Finally, we introduce a simulator and a numerical model to provide a real-time simulation of the soft robotic snake. With the help of the real-time simulator, it is possible to develop and test new locomotion gaits for the soft robotic snake within a short period of time, compared to experimental trial and error. As a result, the soft robotic snake presented in this paper is able to locomote on different surfaces, perform different bio-inspired and custom gaits, and climb over steps.

Keywords: Soft Snake Robot, Pneumatics, Bioinspired Locomotion, Soft Robot Simulation

1. Introduction

Mobile robots are promising tools for emergency response. However, it is not easy for traditional rigid robots to explore narrow, complicated, unknown, or dangerous environments, especially where first responders cannot enter during search-and-rescue missions.

Snake robots may be a solution for traversing these complicated environments. As very flexible and agile creatures, biological snakes evolved to move efficiently in different kinds of terrains because of their unique structure and locomotion gaits. In addition, the softness of snake bodies increase their adaptability and flexibility which makes them compliant to contact with the environment. These features make snake-inspired robots suitable for search-and-rescue missions in uncertain and constrained environments.

This article presents the design, fabrication, verification, and real time simulation of a modular 3D soft robotic snake based on the 2D pneumatic snake robot we introduced previously.[1] With 3-degree-of-freedom (DoF) modules, the proposed snake robot can perform three-dimensional (3D) locomotion instead of simply planar motion. Three different locomotion methods, lateral undulation, sidewinding locomotion, and step climbing, are presented and tested on different surfaces and with different numbers of modules. A simulation environment was developed in parallel using NVidia Flex, which is a particle-based simulation technique developed by NVidia Gameworks.

Snake robots have been created with traditional rigid structures. Hirose et al.[2] studied the

*Zhenyu Wan, and Yinan Sun contributed equally to this work.
†The authors are with WPI Robotics Engineering Department. Please address all correspondence to cdonal@wpi.edu.
‡Conflicts of Interest: None.

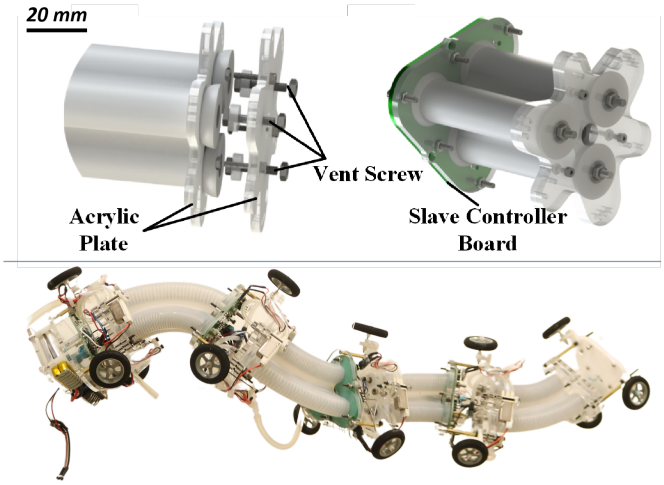

Figure 1. Single module of soft snake robot (top); Soft snake robot (bottom).

kinematics of snake motion and developed multiple snake like robots with active or passive joints and wheels. Choset's research group[3–6] developed a rigid modular snake actuated by servo motors mounted in series, which is capable of multiple gaits including climbing up inside a wall opening and raising its head to observe the environment behind an obstacle. Gravdahl's research group developed an underwater snake robot, propelling with eel like locomotion. Crespi and Ijspeert et al.[7,8] developed a rigid snake robot actuated with DC motors. This robot can conduct planar locomotion with CPG (central pattern generator) on land and swim in water. Transeth et al.[9–11] developed a snake robot "Aiko", which can do obstacle-aided locomotion in addition to frequently used locomotion methods like lateral undulation and sidewinding gaits. In order to increase adaptive functionality to complex terrain, Kano et al.[12] developed a decentralized control scheme which enables the robotic snake to generate reasonable locomotion depend on surrounding environment.

Existing rigid snake robots are actuated using electrical motors and many discrete joints to approximate snake locomotion. However, this discretization with rigid joints is different from the continuous deformation of a biological snake. It requires many more segments of rigid links to create a close approximation of the body motion, which results in more weight, complexity in coordination of the redundant degrees of freedom, and increased energy consumption. In addition, rigid links have to be as short as possible to make sure they don't jam in tight corners, which reduces movement options for a rigid snake, particularly in narrow places.

Our previous work presented a pneumatic soft robotic snake,[13] which can conduct planar continuum lateral undulatory locomotion. Similar to other soft robots,[14–16] our soft-bodied snake robot results in much more flexible, adaptive, and safe motion, emphasizing its potential as a search-and-rescue robot. Pioneering works[17] demonstrated a three chamber structure pneumatic actuator able to bend in three dimensions. With similar structure, we design and fabricate a 3-D soft robotic snake. In order to create anisotropic friction, which is necessary in serpentine locomotion, we utilize passive wheels. Godage's research group[18] designed a soft robotic snake without passive wheels, and fulfill the propulsion by inward and outward rolling locomotion. However the velocity is limited, and the system require a considerable number of tethering tubes for pressure input. Another research work[19] utilize kirigami pattern to create a novel "snake skin", able to create anisotropic friction for snake like robot. However for our snake structure, it is difficult to come up with a skin cover without eliminate the performance. We also developed a composite silicone rubber material to improve the robustness of 3-D snake robot modules to increase their bending amplitude and performed preliminary tests with lateral undulation and sidewinding gaits of an early version of a 3-D soft robotic snake comprising 4 of these modules.[13] In a separate study, we studied soft hybrid wave-spring actuators,[20] used for soft manipulation systems to be able to carry large payloads without buckling. Based on these prior results, we present in this article new soft snake modules with wave-spring sheaths to develop a novel 3-D soft mobile robot that can raise its head over obstacles and traverse over steps without buckling for the first time.

These new capabilities enable a broad range of new gaits and motions for a soft robotic snake. The design space is vast for trial-and-error experimentation. This motivates the requirement for a convenient simulator of our system which would let us quickly design and test potential gaits. For rigid mobile robots, real-time simulations are easily performed using existing simulator tools, while for soft mobile robots with deformable structures, real-time simulation is an active research area because of the limitations in current simulation methods. Huang et al.[21] developed a discrete differential geometry based numerical simulation method for limbed soft robots. The computational efficiency of this method enables it to fulfill real-time simulation for a star-shaped rolling robot. Duriez[22] presented a real-time finite element method (FEM) based simulation and used it as a part of the controller to control a 3-D silicone rubber soft robot inspired by a parallel motion platform. In recent work, we explored the potential of NVidia Flex as a real-time simulator for soft snake robots in 2-D only.[23] This system provides a powerful tool to seamlessly simulate hyper-elastic structures and rigid bodies. Building on our experience, we present a real-time simulator prototype in this article, based on NVidia Flex to simulate our 3-D soft robotic snake, which is a much more complicated soft robotic system. We use this method to build a real-time simulation and help us quickly develop and test new locomotion gait patterns for our soft robotic snake. To demonstrate the power of this method, we present experimental results that lets the robotic snake to go over a 7 cm step using a a custom locomotion gait first generated in simulation and directly utilized in the real world without modification.

Contributions of this work include:

- We present a 3D soft robotic snake with
  - a modular system architecture comprising identical modules with integrated 3D soft actuation, valving, and electronics;
  - wave-spring sheaths that enhance the resistance against buckling and twisting when the snake modules are under large external forces.
- We demonstrate and verify different locomotion gaits and methods with the 3D soft robotic snake prototype, including
  - Lateral undulation,
  - Sidewinding locomotion, and
  - A novel step climbing locomotion which is developed in the real-time simulation conveniently and rapidly as compared with experimental iterations.
- We present a real-time simulation for this complex pneumatic soft robotic system to provide an intuitive environment for more flexible design and assessment of various gaits with significant advantages of developing and testing in a rapid pace.

This article is organized as follows: In Section 2, we describe the design and fabrication methods of our soft robotic snake and wave-spring sheath; In Section 3, we demonstrate three different locomotion gaits with our proposed soft robotic snake platform, and we compare the locomotion path with our simulation results; In Section 4, we conclude this article with a discussion and future research directions; In the Appendix, we add more details about the GPU-based NVidia Flex simulator.

2. Materials and Methods

2.1. Modular Design

Our 3D soft robotic snake incorporates a modular architecture based on our previous prototypes,[13] as shown in Figure 1. Dimension of a 4 segments modular soft robotic snake is listed in Table 1 Modular design allows broken modules to be easily replaced and repaired separately, increasing the maintenance efficiency and system reliability. In addition, the modular design makes it possible to scale the number of the modules, which would provide redundancy. A greater number of modules is helpful especially for step climbing experiments.

Each module consists of a pneumatic silicone

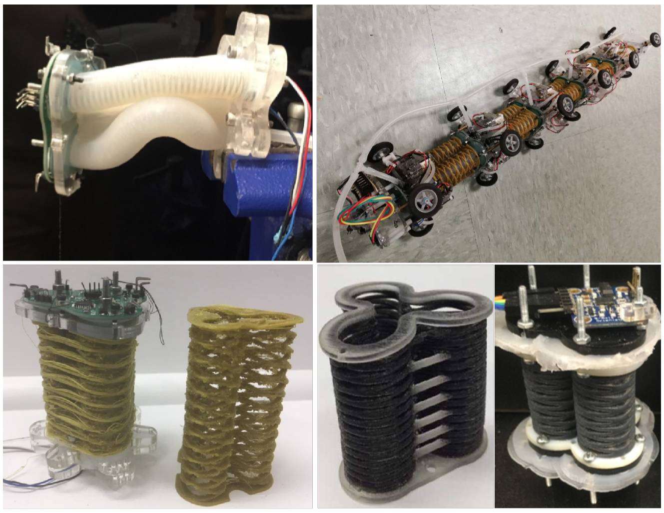

Figure 2. Top-left: An example of a soft robotic module buckling in a cantilever configuration. The lower actuation chamber is pressurized while a downwards force is applied to the tip; Bottom-left: A fully integrated module and the wave spring sheath 3-D printed out of NinjaFlex; Top-right: Snake robot made of five modules with NinjaFlex sheaths mounted; Bottom-right: Wave spring sheath with and without horizontal support 3-D printed out of Objet FLX9085.

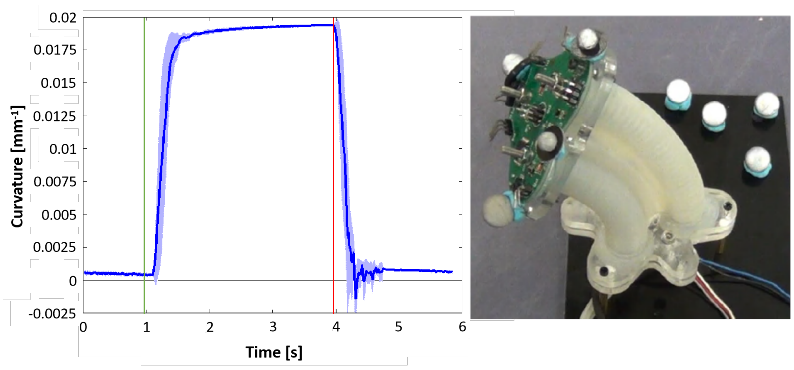

Figure 3. Left: Inflation and deflation curve with shaded error region. (the green line represent the time when signal input is applied, and the red line represent the end of the signal input). The inflation pressure is 17 psi. Right: A bending module in testing.

rubber soft bending body with three embedded chambers, three solenoid valves and a peripheral controller printed circuit board (PCB). The three valves control the air flow of the three chambers independently and the states of the valves are controlled by the peripheral controller. A main controller mounted in the head module connects to the peripheral controllers through an I^2C communication bus to send desired values of valve duty cycles mapped from the target pressure. Peripheral controllers operate the solenoid valves with a PWM signal according to the received duty cycle, so that the chambers in each module can be actuated with a corresponding pressure.

2.2. *Wave Spring Sheath Constraint*

Under unexpected external forces, silicone rubber modules will buckle even if silicone with relatively high elastic modulus is used, which limits the performance of soft robots. As shown in Figure 2 (left), the pressurized chamber buckles, elongating without bending the entire module. This limits the ability of the soft robotic snake to traverse obstacles and perform complex gaits or motions in 3-D. For example, when performing step climbing locomotion, soft robotic snake modules buckle under the influence of gravity. As a result, locomotion can not be performed as desired, reducing the maximum height the soft robotic snake can traverse.

We address this problem by encasing the snake modules in 3D-printed wave springs based on our

Table 1. Dimension of a 4 segments modular soft robotic snake.

Parameter	Value (mm)
Module length	70
Height	100
Inner chamber diameter	8
Passive wheel diameter	20
Total length	510

previous research.[20] Wave springs consist of a stacked series of flexible waves and are traditionally used in applications where a traditional coil spring may be too large. We utilize this type of flexible wave in order to have a sheath for the snake module that can selectively extend, allowing the module to bend, while also resisting buckling. Flexible 3D printing allows us to modify this structure to conform to the contours of the bending modules, and we add horizontal supports to further resist buckling.

We made two different designs of sheaths shown in Figure 2, with two different materials, Objet FLX9085 and NinjaFlex. We observed that the Objet FLX9085 wave springs were expensive and prone to breakage while NinjaFlex wave springs were more reliable and more elastic.

2.3. System Architecture

The 3D soft robotic snake is a modular robot composed of at least three soft robotic modules mounted in series. The modules are connected with screws and spacers, as well as wires, tubes and passive wheels located in short gaps between adjacent modules. We mount the main controller, an Arduino Pro Mini with Atmega328 chip, at the head of the soft robotic snake. Two 2-cell lithium polymer batteries (the voltage is 7.4 V) are mounted at the head and the tail respectively, to power the control circuit and the valves and maintain balance. In addition, we add a Bluetooth module on the main controller to enable remote commands to switch between locomotion modes.

3. Results

3.1. Motion Capabilities of Soft Robotic Modules

We first performed experiments to evaluate the 3-D soft robotic modules for their ability to generate the desired motions and to withstand reasonable external loads for realistic locomotion gaits of a 3-D soft robotic snake.

3.1.1 Inflation and deflation : Thirty sets of experiments are conducted to test the inflation and deflation performance of the modules in bending, which provides us with dynamic response information relevant for the bending waves used in the locomotion gaits. During the experiments, the soft robotic module is inflated to bend in a step response, then deflated to recover after a certain amount of time, following a square wave pattern. Figure 3 shows the mean inflation and deflation curve with the shaded region representing standard deviation between experiments. Based on these experiments, we quantify the inflation and deflation time constants as between 0.23-0.44 s. In order to fully inflate and deflate the chambers as possible, for each chamber it would take 0.46-0.88 s. Thus we confine the gait frequency in the locomotion experiments to be no higher than 2 Hz, so that there is a reasonable chance for the actuators to be fully actuated.

3.1.2 Hexagonal Gait : In order to achieve sidewinding locomotion, the soft robotics modules should bend such that their end-plates (tips) move in circular paths with a desired phase delay between adjacent modules. For ease of implementation and to increase computational efficiency, we approximate this ideal circular gait and develop a hexagonal gait which can be simply implemented by binary inflation-deflation for each actuation chamber without controlling the pressure which would be required to achieve precise circular tip trajectories. Figure 4 shows that the tip trajectory of the modules performing the hexagonal gait is tracing a deformed hexagon projected on the spherical workspace of the module.

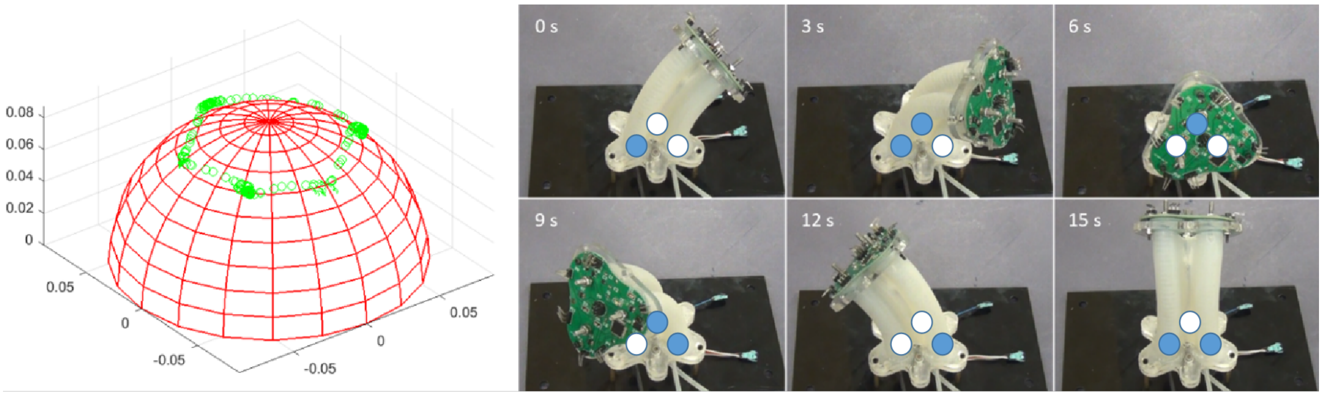

Figure 4. Left: Green datapoints represent the trajectory of the central point at the top end-plate (tip) of the module when performing the hexagonal gait. The trajectory, which also can be considered as the workspace, is a deformed hexagon on a (red) spherical. Right: A soft robotic module in testing. The blue and white dots show the status of the three actuation chambers. Blue dots mean inflated states and white dots mean deflated states.

3.1.3 Wave Spring Sheath: The goal of adding the custom flexible wave spring sheaths to the soft robotic modules is to increase the resistance to buckling under external force. We set up experiments to test the wave spring sheaths. A bending module with different kinds of custom wave spring sheaths mounted is set in a cantilever configuration with a downward tip load as shown in Figure 2 (Left). We gradually increase the pressure in the lower actuation chamber, and measure the maximum module height and bending angle it can reach before buckling. As shown in Figure 5, the sheaths have significant effect on reducing buckling when pressurized actuators are under external force. In addition, the Objet sheath with horizontal supports is generally the best performer. However, under higher loads, it performs similar to the NinjaFlex sheaths. Given the advantage in cost and reliability of the NinjaFlex sheaths, we select the NinjaFlex Sheath as the best choice.

3.2. Locomotion Capabilities of the Modular 3-D Soft Robotic Snake

In this section, we connect 4 bending modules in series to create a robotic snake and test undulatory and sidewinding locomotion on it. Also we test custom step climbing locomotion gaits on an enhanced version of robotic snake with an additional module and wave-spring sheath constraint structure for improved ability to resist gravitational forces during climbing. The robotic snake use low-level valve duty cycle commands that vary along the length of the robot according to desired functions or algorithmic sequences that generate the specific gaits. For undulatory and sidewinding locomotion, we use four modules in the soft robotic snake prototype to reduce overall length. For step climbing locomotion, we use five modules to increase the propulsion and balance of the body during lift off. The experiments are conducted with varying settings to study their effect in locomotion performance. We use a motion capture system to record the trajectory of the soft robotic snake. In parallel, we conduct the simulation studies under the same settings and compare the simulation results with the experimental results in the real world.

3.2.1 Undulatory Locomotion: Undulatory locomotion is a well known locomotion gait of biological snakes, which is also easily conducted by many robotic snakes. With a bidirectional bending motion in the horizontal plane, the snake thrusts its body from side to side, creating a travelling wave, and propels itself with the effect of anisotropic friction provided by snake scales. On our soft robotic snake, the anisotropic friction is provided by the passive wheels mounted on the robot and the motion pattern is identical to the one observed in biological snakes. To perform undulatory locomotion, all the modules undergo bidirectional bending with a certain phase delay between adjacent modules creating a traveling wave of curvature. To generate this motion, we use Equation 1 to control the robotic snake (K_{ij} describes

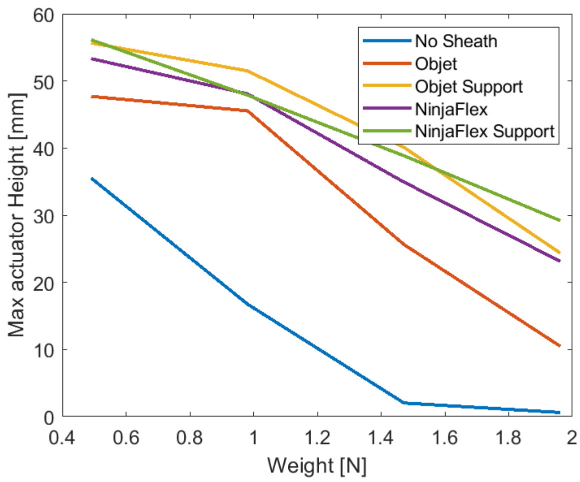

Figure 5. The max tip height achieved by the bending module in cantilever configuration under tip loading. With reduced buckling effect, the actuators bends higher.

the status of each channel in segments. ω and β refer to the frequency and phase delay in the gaits. Detailed description of the parameters are shown in Table 2).

$$K_{ij} = sgn(sin(2\pi\omega t + i\beta + j\pi) + \phi),\quad i \in (0, 1, 2...N-1), j \in (0, 1). \tag{1}$$

During this locomotion, we do not actuate the top chamber in each segment. Geometrically, if we would like to make sure the segment bending on the same surface, it is needed to "half actuate" the top chamber. While in the real world experiment, the bending on upward direction will be largely reduced by gravity. As the result, the lateral undulation will stay on the same plane.

We conduct experiments to demonstrate undulatory locomotion on a paper surface with frequency (ω) of 1.5 Hz, 1.75 Hz, and 2 Hz. The phase delay is set to be $2\pi/3$, which results in 1.25 traveling curvature waves along the body. For comparison, the same tests are conducted in the real-time simulation for our soft robotic snake. In Figure 6, the trajectory of the soft robotic snake CoM (central of mass) are presented. The blue lines represent the result from simulation, while the red lines represent the result from real world experiments. In real world experiment, the robotic snake robot can reach velocity of 140.25 mm/s (0.275 body length/s) under 2 Hz.

The robotic snake is theoretically supposed to move in a straight line with constant input and parameter setting. Because of the fabrication inaccuracy, uneven paper surface, and unexpected sliding friction, the robotic snake can not move in a straight line. The simulation results present a similar tendency and velocity with the real world experiments, while the trajectories in simulation results are closer to a straight line since there are no fabrication inaccuracies and the surface can be set to be perfectly even. Deviation in simulation is caused by noise added in contact calculation, and the model for hyper-elastic material is simplified for calculation efficiency, which result in error under large deformation, thus the simulation shows some deviation. Higher frequency have little effect on simulation results, while in real world experiments, higher frequency causes more unexpected sliding during undulatory locomotion, thus the deviation increases. Our previous work presents a method to fulfill trajectory following for soft robotic snakes with an iterative learning controller.[24] While in this work, in order to test the performance of the soft robotic snake and compare with the simulation, we do not add any controller during the experiments.

3.2.2 Sidewinding Locomotion : Sidewinding is a variation of the serpentine motion that makes use of all 3 degrees-of-freedom in each segment. It physically lifts parts of its body off the ground, giving the body an S-shape with two points of contact with the ground to push the snake in a diagonal direction. Sidewinding locomotion utilizes static friction force instead of sliding on the surface, thus it may have the advantage of higher en-

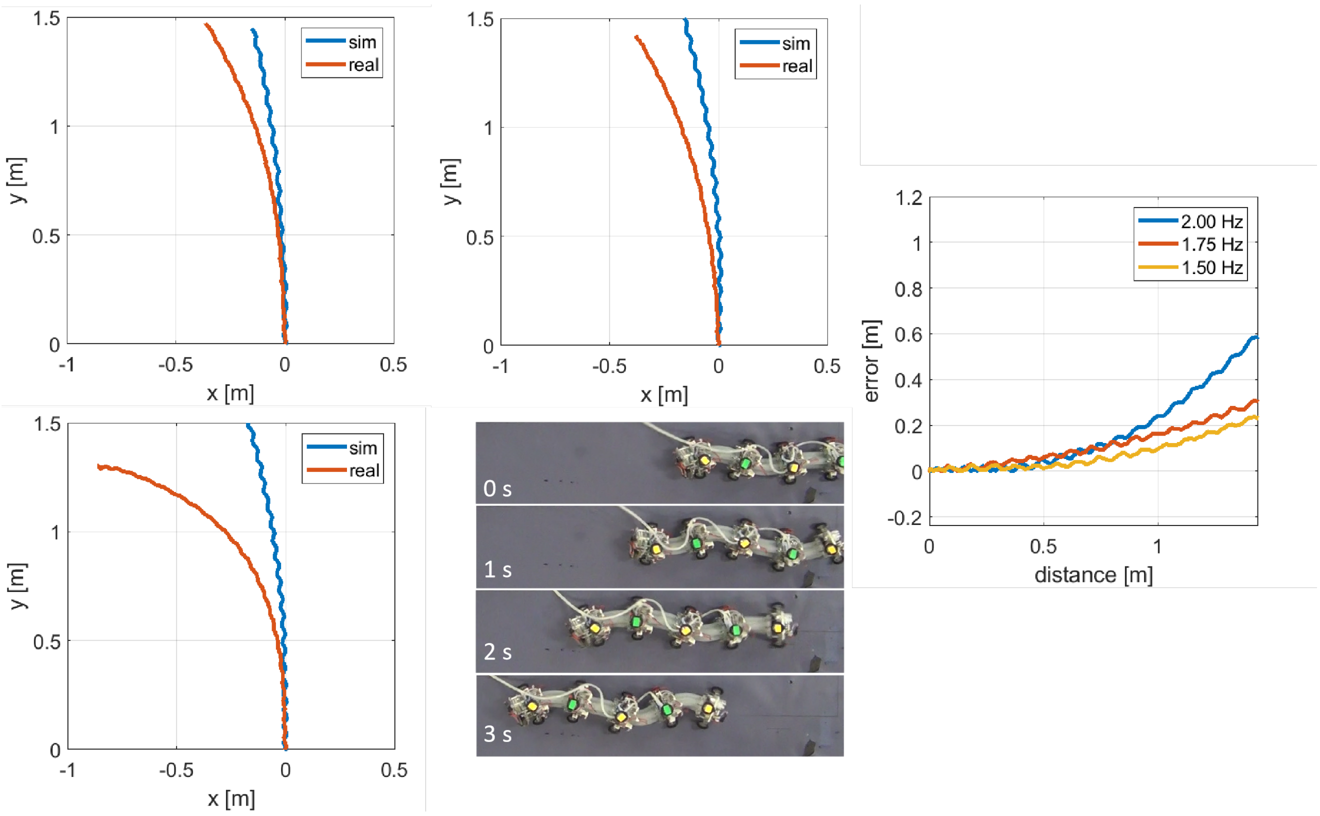

Figure 6. Top-Left: Trajectory of the soft robotic snake CoM (central of mass) when locomotion frequency is 1.50 Hz. Top-Middle: Trajectory of the soft robotic snake CoM when locomotion frequency is 1.75 Hz. Bottom-Left: Trajectory of the soft robotic snake CoM when locomotion frequency is 2.00 Hz. Bottom-Middle: Soft robotic snake performing lateral undulation locomotion from right side to left side in real world. Right: Error between simulation result and real world experiment result with relate to distance traveled.

ergy efficiency, but spends energy against gravity to lift the body up. As discussed in Section 3.1.2, To realize this locomotion gait in the soft robotic snake, we developed a hexagonal gait to approximate the circular bending motion observed in biological snakes. In order to conduct the locomotion, we use Equation 2 to control the soft robotic snake (K_{ij} describes the status of each channel in segments. ω and β refer to the frequency and phase delay in the gaits. Detailed description of the parameters are shown in Table 2).

$$K_{ij} = sgn(sin(2\pi\omega t + i\beta + j\frac{2\pi}{3}) + \phi), \quad i \in (0, 1, 2...N-1), j \in (0, 1, 2). \tag{2}$$

We conduct experiments to demonstrate sidewinding locomotion on a paper surface with frequency (ω) of 0.75 Hz, 0.875 Hz, and 1 Hz. The phase delay (β) is set to be $\pi/2$, which results in one full traveling curvature wave along the body. For comparison, the same tests are conducted in the real-time simulation for our soft robotic snake. In Figure 7, the trajectory of the soft robotic snake CoM (central of mass) are presented. The blue curves represent the simulation results, while the red lines represent the results from real world experiments. In real world experiment, the robotic snake robot can reach velocity of 76.50 mm/s (0.150 body length/s) under 0.875 Hz.

Compared to lateral undulation locomotion, sidewinding locomotion has better fit between simulation and experimental result. When performing sidewinding, the segments on robotic snake was applied with extra force from gravity and ground compared to lateral undulatory locomotion, result in lower deformation. Meanwhile, the model for hyperelastic material is set to be low order Mooney-Rivlin inside the simulator as a trade off between efficiency and accuracy. As a result, the simulator has a better fitting of lower hyperelastic material deformation which happened in sidewinding locomotion and the step climbing locomotion.

Table 2. Parameters of gait functions.

Symbol	Description
i	sequence of the segment(0 represents the 1^{st} segment)
j	sequence of the channel(0: bottom left; 1: bottom right; 2: top)
K_{ij}	status of j^{th} channel in i^{th} segment(-1: deflation; 0: stay still; 1: inflation)
ω	frequency of the undulation gait
t	total running time
β	phase difference between adjacent segments
ϕ	offset of the travelling wave
N	number of segments

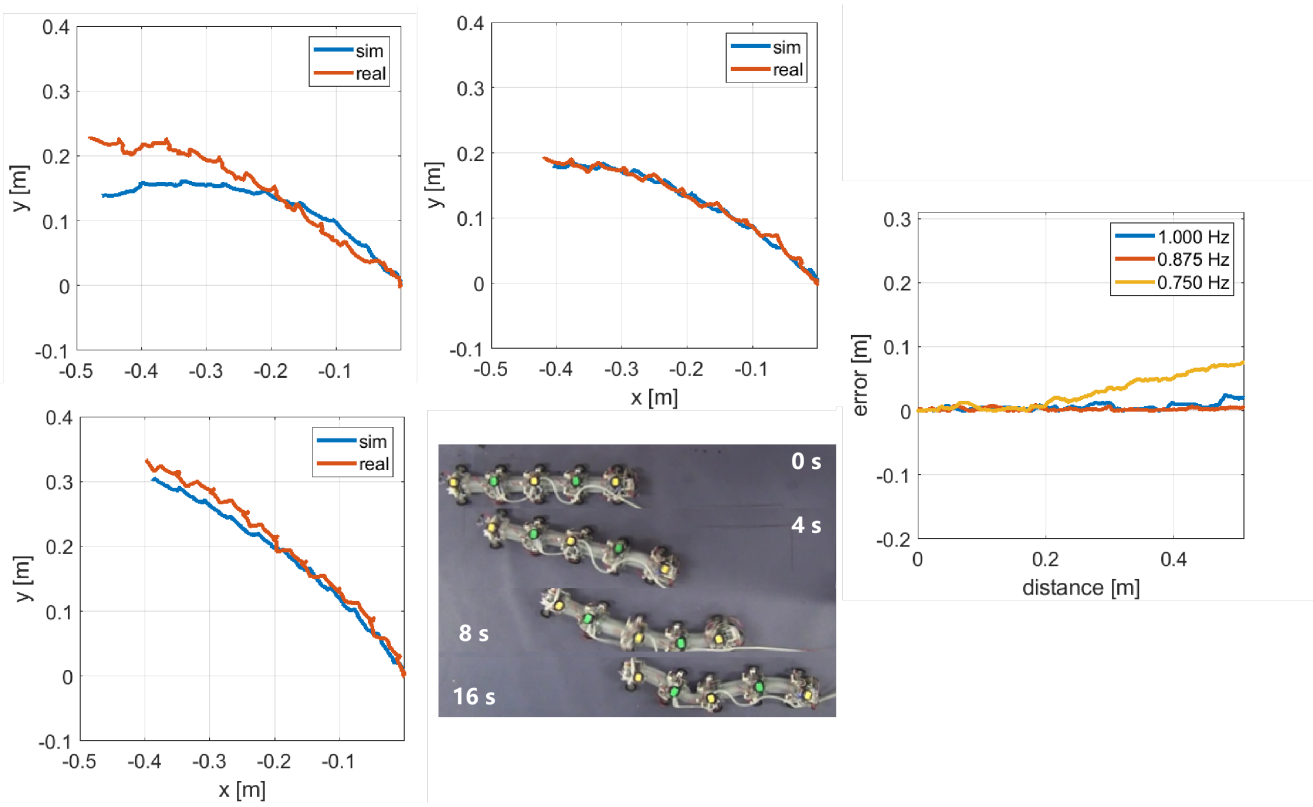

Figure 7. Top-Left: Trajectory of the soft robotic snake CoM (central of mass) when locomotion frequency is 0.75 Hz. Top-Middle: Trajectory of the soft robotic snake CoM when locomotion frequency is 0.875 Hz. Bottom-Left: Trajectory of the soft robotic snake CoM when locomotion frequency is 1.00 Hz. Bottom-Middle: Soft robotic snake performing sidewinding locomotion on a paper surface. Right: Error between simulation result and real world experiment result with relate to distance traveled.

Since sidewinding locomotion is a 3 dimensional, contact based locomotion, there is seldom unexpected sliding compared to undulatory locomotion, also, the effects of surface variations are reduced. As a result, our simulation results are more similar to our real-world experimental results.

3.2.3 Step Climbing Locomotion : To explore the proposed 3-D soft robotic snake's ability to operate on non-planar environments, we developed a custom locomotion sequence based on the climbing motion of real snakes, which allows our robot to climb up a step. At least three modules are needed on the ground for the robot to perform snake-like lateral undulation locomotion and power the robot to move forward. The step climbing motion will result in intermediate states with several modules that can not touch the ground when climbing up high steps due to the restriction of the module length. Thus, in order to gain higher thrust and better balance we added one

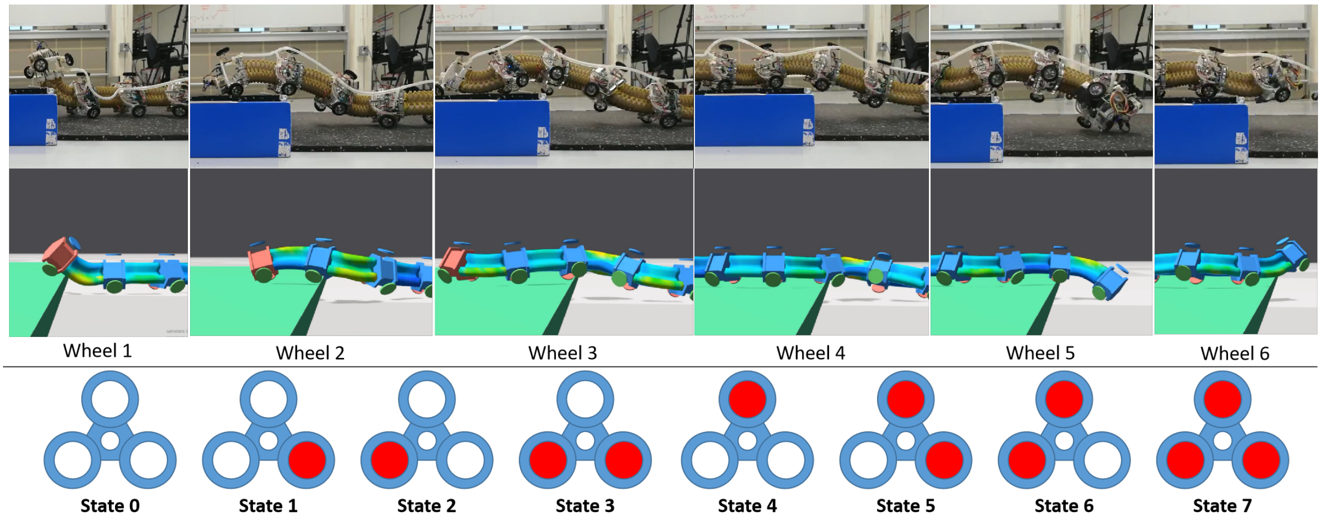

Figure 8. Step climbing in real world experiment (top) and in real-time simulation (center). Bottom: Actuation States of the proposed soft robotic modules. Each subplot displays the cross-section of the soft module with three pneumatic chambers around a central slot for wiring. Red chambers are pressurized, and white chambers are depressurized.

Table 3. State of each segment to lift each wheel in step climbing locomotion. "/" means switching, for example, "2/1" means switching between state 2 and state 1 under the frequency of ω. The states are explained in Figure 8.

	segment1	segment2	segment3	segment4	segment5
wheel1	3	2/1	2/1	2/1	2/1
wheel2	4	4	2/1	2/1	4
wheel3	2/1	4	3	2/1	2/1
wheel4	2/1	2/1	4	3	2/1
wheel5	2/1	2/1	2/1	4	4
wheel6	5/6	2/1	2/1	2/1	3

more module to the robot, and created this gait for a 5-module version of the robotic snake, without loss of generality. As a result, this version offers greater balance for some of the modules to be lifted off the ground.

The snake modules are strong enough for lateral undulation and sidewinding locomotion. However, when lifting themselves off the ground, the external force applied on each segment would easily result in buckling, thus the original soft robotic snake in our previous work fails to climb up. This task exemplifies the need for engineering directional stiffness for soft robots, enabling a level of rigidity in some directions and compliance in others. We achieve this anisotropic stiffness response with a flexible 3-D printed sheath as discussed in Section 3.1.3, which significantly improves the performance in step climbing, as determined previously through individual module experiments.

In order to climb on a step, we need a specific locomotion gait developed as we have done for undulatory and sidewinding locomotion. Instead of trial and error in real-world experiments, we tested and adjusted possible gaits in our real-time simulation. By creating extra constraint with corresponding parameters in the simulator, the snake robot in simulation has similar anti-buckling performance with the soft robotic snake mounted with 3D printed sheath (as shown in Figure 8) in real world. With the help of our simulator, a group of gaits are developed to make sure our snake robot can climb on a 7 cm step, which we set as a challenge since it is as high as the snake itself. The step climbing locomotion gait is described in Table 3 and Figure 8.

In the process of climbing up a step, the robot first moves forward with its head (first module) raised up (bending upwards). After the passive wheels of the first module land steadily on the step, the first module bends downward to get a foothold force and raises the second module while the rest of the body follows lateral undulation to continue pushing forward. After the passive wheels of the second segment land steadily on the step, the head module resumes its regular lateral undulatory serpentine locomotion to move forward, while the second module bends downward in order to avoid slipping backward. Meanwhile, the third module is lifted up to repeat the same procedure as the second module. After landing on the ground of the upper step steadily, the third module can return to its normal serpentine locomotion and lift the tail part of the robot. With the rest of the modules pulling it forward with lateral undulation, the tail can land on the upper step easily. This gait essentially generates a simple vertical wave that travels once from head to tail on top of the generic lateral undulation gait which continues pushing the body forward, revealing an interesting way to fuse gaits for 3D motion enabled by our 3D soft robotic modules.

4. Conclusion

In this paper, a 3D soft robotic snake and accompanying 3D-printed wave spring sheath are designed, fabricated, and validated. Experiments were performed to test the performance of a single soft robotic module, as well as the locomotion of the snake robot under undulation and sidewinding gaits. A simulation platform based on NVidia Flex was developed and verified using experiments on the physical snake. Developing a step climbing gait, we were able to command the 3D soft robotic snake to traverse a 7 cm high step, demonstrating its ability to function in non-planar environments for the first time, while showing the ability of the NVidia Flex system to seamlessly simulate robotic systems with hyperelastic structures and rigid bodies in real time. The 3-D printed wave spring can help with the buckling behavior, but can not fully eliminate it which still restricts the ideal climbing capability, we will extend our current design advantages and keep researching better structures to address this issue.

Our real-time simulation presents a way to generate reliable information quickly, especially for gait development. The soft robotic snake is a complex pneumatic hyperelastic system to simulate. In order to fulfill real-time simulation requirements, there is a trade-off between computational complexity and accuracy of the results. The ability of the NVidia Flex platform to use GPU based computation is very beneficial for our simulations. We measured that the simulation speed has increased about 30% recently because of the steadily increasing performance of new GPU hardware. In future work, we will keep exploring the potential of simulations based on Nvidia Flex, and plan to implement different models for hyperelastic materials to increase the application and accuracy of the real-time simulation for any soft robotic system.

In addition, future work will extend our snake-like mobility platforms to operate in the field, addressing challenges in perception, data analysis, power autonomy, and range of motions toward a universal mobility platform useful in real-world applications such as search and rescue in complex environments.

5. Appendix

5.1. Nvidia Flex based simulation

The 3D robotic snake is simulated using a particles and rigid bodies system derived from Lagrangian multi-physics mechanics, given in the general form as Equation 3 that includes external and gyroscopic forces.

$$\begin{gathered} M\ddot{q} - f(q,\dot{q}) - J_b^T\lambda_b - J_n^T\lambda_n - J_f^T\lambda_f = 0 \\ c_b(q,p) + E\lambda_b = 0 \\ 0 \le c_n(q) \perp \lambda_n \ge 0 \\ \forall i \in A, D_i^T\dot{q} + \frac{|D_i^T\dot{q}|}{\lambda_{f,i}}\lambda_{f,i} \ge 0 \\ \forall i \in \mathcal{J}, \lambda_{f,i} = 0 \end{gathered} \tag{3}$$

Interactions between particles are defined as a set of bi-lateral and unilateral constraints (c_b and c_n, respectively), and are associated with their respective Lagrange multipliers λ_b and λ_n. With the use of a compliance (or inverse stiffness) term defined in the block-diagonal matrix $E \in R^{n_b \times n_b}$, bilateral constraints can be used to store elastic energy potentials, as described in Backman et al.[25] The target pressures for the link modules are included in the vector p, which are parameters for a select set of bilateral constraints to simulate the resulting expansion of the links. The contact and frictional forces are based on Coulomb's model, which defines an admissible cone of contact forces,[26] and defined by the unilateral contact constraints, and μ_i the friction coefficient for the i^{th} contact. The frictional forces for a contact are parameterized by $\lambda_{f,i}$, with a corresponding basis D_i defining the surface tangent plane at the contact point. Active contacts are defined in the set $A = i \in (1, ..., n_c)|\mu_i \lambda_{n,i} > 0$ with inactive contacts $\mathcal{J}$ being its complement. The constraint Jacobians J_b, J_n contain the gradient of bilateral and normal constraint functions with respect to q, and we define the set of frictional basis vectors as the matrix $J_f = [D_1, ..., D_{n_c}]^T$. Tetrahedral finite-elements are used to model the solid chamber material. Assuming a constant strain element and a linear isotropic constitutive model, each tetrahedron defines a 6-dimensional bidirectional constraint vector,

$$c_{tetra} q + E_{tetra} \lambda = 0 \tag{4}$$

where $c_{tetra}(q) = [\epsilon_{xx}, \epsilon_{yy}, \epsilon_{zz}, \epsilon_{yz}, \epsilon_{xz}, \epsilon_{xy}]$ is the vector of corotational strains in Voigt notation, and E_{tetra} is the constant element compliance matrix, given by:

$$E_{tetra} = \frac{1}{V_e Y} \begin{bmatrix} 1 & -v & -v & 0 & 0 & 0 \\ -v & 1 & -v & 0 & 0 & 0 \\ -v & -v & 1 & 0 & 0 & 0 \\ 0 & 0 & 0 & 1+v & 0 & 0 \\ 0 & 0 & 0 & 0 & 1+v & 0 \\ 0 & 0 & 0 & 0 & 0 & 1+v \end{bmatrix} \tag{5}$$

Where V_e is the element volume, Y and v are the material Young's modulus and Poisson's ratio, respectively.

5.1.1 Pressure Dynamics : In order to simulate the pressure on the chambers, since each chamber is constrained by a helical thread wound around its axis,[13,27] the only direction available for expansion is along the axis. Therefore, the bilateral constraints on the axis direction for particles that make up the cavity receive an actuation parameter based on the pressure applied. Since the elastic model used is linear with stress, the expansion ratio with the pressure is given with respect to the rest pose by the factor $\epsilon(p)$ as: $\epsilon(p) = 1 + \frac{p}{Y}$ Given the limited airflow provided by the valves, the pressure delivery must obey the following relationship given by:

$$v^2 = \frac{2}{\rho}(p - p_s) \tag{6}$$

Where ρ is the air density p is the target pressure in the chamber, p_s is the source pressure, and v is the air flow to the chamber. This results in the following discrete time update equation:

$$\Delta p_i = \frac{p_i(t+h) - p_i(t)}{p_s} \tag{7}$$

Where t is the current time, p_i is the pressure in chamber at current simulation step, and h is a fixed time step. Each time-step performs 4 iterations of Newton's method, with each linear system solved approximately using 20 Preconditioned Conjugate Residual (PCR) iterations to ensure a fixed computational cost. The chamber deflates in an isobaric curve, until its volume ceases to reduce, then slowly releasing the remaining air until stabilizing with atmospheric pressure. Therefore the deflation ratio is limited to a threshold T_p, resulting in the following differential equations for pressure update:

$$p_i(t+h) = \begin{cases} p_i(t) + p_s \Delta p_i^2 k_i, & \text{inflating;} \\ p_i(t) - min(p_i(t) k_d, T_p), & \text{deflating.} \end{cases} \tag{8}$$

Where k_i,k_d are the inflation and deflation damping parameters respectively, tuned according to experimental data for the link.

5.1.2 Buckling effect : Just like in the real soft modules, the effect of adding pressure on the simulated modules causes buckling of the expanded chamber, due to forces pushing against it. In order to avoid buckling to reproduce the effect of the proposed wave-spring sheath, a set of constraints were added to replicate the behavior of the sleeve. Stiff bidirectional constraints were added between particles that make up the exterior wall of each chamber, such that it won't let one chamber to buckle against another.

Acknowledgments

This material is based upon work supported by the National Science Foundation (NSF) under Grant Nos. IIS-1551219, CMMI-1728412, and CMMI-1752195. Any opinions, findings, and conclusions or recommendations expressed in this material are those of the authors and do not necessarily reflect the views of the NSF.

References

[1] M. Luo, Y. Pan, E. H. Skorina, *et al.*, "Slithering towards autonomy: a self-contained soft robotic snake platform with integrated curvature sensing," *Bioinspiration & biomimetics*, vol. 10, no. 5, p. 055001, 2015.

[2] S. Hirose and H. Yamada, "Snake-like robots [tutorial]," *IEEE Robotics & Automation Magazine*, vol. 16, no. 1, pp. 88–98, 2009.

[3] C. Wright, A. Johnson, A. Peck, *et al.*, "Design of a modular snake robot," in *2007 IEEE/RSJ International Conference on Intelligent Robots and Systems*, pp. 2609–2614, IEEE, 2007.

[4] C. Wright, A. Buchan, B. Brown, *et al.*, "Design and architecture of the unified modular snake robot," in *2012 IEEE International Conference on Robotics and Automation*, pp. 4347–4354, IEEE, 2012.

[5] H. Marvi, C. Gong, N. Gravish, *et al.*, "Sidewinding with minimal slip: Snake and robot ascent of sandy slopes," *Science*, vol. 346, no. 6206, pp. 224–229, 2014.

[6] J. C. McKenna, D. J. Anhalt, F. M. Bronson, *et al.*, "Toroidal skin drive for snake robot locomotion," in *2008 IEEE International Conference on Robotics and Automation*, pp. 1150–1155, IEEE, 2008.

[7] A. J. Ijspeert and A. Crespi, "Online trajectory generation in an amphibious snake robot using a lamprey-like central pattern generator model," in *Proceedings 2007 IEEE International Conference on Robotics and Automation*, pp. 262–268, IEEE, 2007.

[8] A. Crespi and A. J. Ijspeert, "Amphibot ii: An amphibious snake robot that crawls and swims using a central pattern generator," in *Proceedings of the 9th international conference on climbing and walking robots (CLAWAR 2006)*, no. CONF, pp. 19–27, 2006.

[9] A. A. Transeth, P. Liljeback, and K. Y. Pettersen, "Snake robot obstacle aided locomotion: An experimental validation of a non-smooth modeling approach," in *2007 IEEE/RSJ International Conference on Intelligent Robots and Systems*, pp. 2582–2589, IEEE, 2007.

[10] A. A. Transeth, R. I. Leine, C. Glocker, *et al.*, "Snake robot obstacle-aided locomotion: Modeling, simulations, and experiments," *IEEE Transactions on Robotics*, vol. 24, no. 1, pp. 88–104, 2008.

[11] A. A. Transeth, R. I. Leine, C. Glocker, *et al.*, "3-d snake robot motion: nonsmooth modeling, simulations, and experiments," *IEEE transactions on robotics*, vol. 24, no. 2, pp. 361–376, 2008.

[12] T. Kano, R. Yoshizawa, and A. Ishiguro, "Tegotae-based decentralised control scheme for autonomous gait transition of snake-like robots," *Bioinspiration & biomimetics*, vol. 12, no. 4, p. 046009, 2017.

[13] Y. Qin, Z. Wan, Y. Sun, *et al.*, "Design, fabrication and experimental analysis of a 3-d soft robotic snake," in *2018 IEEE International Conference on Soft Robotics (RoboSoft)*, pp. 77–82, IEEE, 2018.

[14] M. T. Tolley, R. F. Shepherd, M. Karpelson, *et al.*, "An untethered jumping soft robot," in *2014 IEEE/RSJ International Conference on Intelligent Robots and Systems*, pp. 561–566, IEEE, 2014.

[15] V. Vikas, E. Cohen, R. Grassi, *et al.*, "Design and locomotion control of a soft robot using friction manipulation and motor–tendon actuation," *IEEE Transactions on Robotics*, vol. 32, no. 4, pp. 949–959, 2016.

[16] E. W. Hawkes, L. H. Blumenschein, J. D. Greer, *et al.*, "A soft robot that navigates its environment through growth," *Science Robotics*, vol. 2, no. 8, 2017.

[17] K. Suzumori, S. Iikura, and H. Tanaka, "Development of flexible microactuator and its applications to robotic mechanisms," in *Proceedings. 1991 IEEE International Conference on Robotics and Automation*, pp. 1622–1623, IEEE Computer Society, 1991.

[18] D. D. Arachchige, Y. Chen, and I. S. Godage, "Soft robotic snake locomotion: Modeling and experimental assessment," in *2021 IEEE 17th*

International Conference on Automation Science and Engineering (CASE), pp. 805–810, IEEE, 2021.

[19] C. Branyan, R. L. Hatton, and Y. Mengüç, "Snake-inspired kirigami skin for lateral undulation of a soft snake robot," *IEEE Robotics and Automation Letters*, vol. 5, no. 2, pp. 1728–1733, 2020.

[20] E. H. Skorina and C. D. Onal, "Soft hybrid wave spring actuators," *Advanced Intelligent Systems*, vol. 2, no. 1, p. 1900097, 2020.

[21] W. Huang, X. Huang, C. Majidi, *et al.*, "Dynamic simulation of articulated soft robots," *Nature communications*, vol. 11, no. 1, pp. 1–9, 2020.

[22] C. Duriez, "Control of elastic soft robots based on real-time finite element method," in *2013 IEEE international conference on robotics and automation*, pp. 3982–3987, IEEE, 2013.

[23] R. Gasoto, M. Macklin, X. Liu, *et al.*, "A validated physical model for real-time simulation of soft robotic snakes," in *2019 International Conference on Robotics and Automation (ICRA)*, pp. 6272–6279, IEEE, 2019.

[24] M. Luo, Z. Wan, Y. Sun, *et al.*, "Motion planning and iterative learning control of a modular soft robotic snake," *Frontiers in Robotics and AI*, vol. 7, p. 191, 2020.

[25] A. Backman, K. Bodin, C. Lacoursière, *et al.*, "Democratizing cae with interactive multiphysics simulation and simulators," in *NAFEMS NORDIC Conference: Engineering Simulation: Best Practices, New Developments, Future Trends, 22-23 May 2012, Gothenburg, Sweden*, 2012.

[26] D. E. Stewart and J. C. Trinkle, "An implicit time-stepping scheme for rigid body dynamics with inelastic collisions and coulomb friction," *International Journal for Numerical Methods in Engineering*, vol. 39, no. 15, pp. 2673–2691, 1996.

[27] E. H. Skorina, M. Luo, W. Y. Oo, *et al.*, "Reverse pneumatic artificial muscles (rpams): Modeling, integration, and control," *PloS one*, vol. 13, no. 10, p. e0204637, 2018.